Icarus 344 (2020) 113460

Contents lists available at ScienceDirect

Icarus

journal homepage: www.elsevier.com/locate/icarus

N_2 and H_2 broadened isobutane infrared absorption cross sections and butane upper limits on Titan

Dan Hewett [a,*], Peter F. Bernath [a], Andy Wong [a], Brant E. Billinghurst [b], Jianbao Zhao [b], Nicholas A. Lombardo [c,d,e], Conor A. Nixon [e], Don E. Jennings [f]

[a] Department of Chemistry and Biochemistry, Old Dominion University, Norfolk, VA 23529, USA
[b] Canadian Light Source Far-Infrared Beamline, 44 Innovation Blvd, Saskatoon, SK S7N 2V3, Canada
[c] Center for Space Science and Technology, University of Maryland, Baltimore County, 1000 Hilltop Circle, Baltimore, MD 21250, USA
[d] Center for Research in Exploration and Space Science Technology, University of Maryland, Baltimore County, 1000 Hilltop Circle, Baltimore, MD 21250, USA
[e] Planetary Systems Laboratory, Solar System Exploration Division, NASA Goddard Space Flight Center, 8800 Greenbelt Road, Greenbelt, MD 20771, USA
[f] Instrument Systems and Technology Division, NASA Goddard Space Flight Center, 8800 Greenbelt Road, Greenbelt, MD 20771, USA

A B S T R A C T

High resolution infrared absorption cross sections of isobutane, $(CH_3)_3CH$, were measured in the 1050–1900 cm^{-1} spectral range by Fourier transform spectroscopy. Four sample temperatures (210, 234, 265 and 296 K) were used with three pressures (10, 30 and 100 Torr) of N_2 and H_2 broadening gas. Spectra of pure isobutane samples were also recorded. These cross sections are useful for the interpretation of infrared spectra of the Giant Planets and Titan. The isobutane cross sections give an upper limit of 3.91e-8 for its fractional abundance on Titan based on CIRS/Cassini infrared spectra. Using *n*-butane, $CH_3(CH_2)_2CH_3$, cross sections from the literature, we obtain an upper limit of 5.13e-7 for its abundance on Titan. The combined upper limit for both isomers of butane, C_4H_{10}, on Titan of 5.52e-7 is consistent with the lower limit of recent model predictions.

1. Introduction

The chemical composition of planetary atmospheres is of great interest. Titan, a large moon of Saturn, has been studied extensively notably by the Cassini-Huygens mission (Coustenis et al., 2007; Flasar et al., 2005; Nixon et al., 2009; Teanby et al., 2007; Vinatier et al., 2007; Vinatier et al., 2010). Titan is the focus of such studies due to its organic-rich atmosphere, primarily small hydrocarbons, nitriles and aerosols ("haze") (Bezard, 2009; Bezard et al., 2014; Lebonnois et al., 2001; Rannou et al., 2003; Trainer et al., 2004; Vinatier et al., 2012). This atmosphere is considered to be similar to that of pre-biotic Earth, and therefore an important system for elucidation of the development of life on Earth (Raulin et al., 1986; Raulin et al., 1984; Trainer et al., 2006).

Titan's atmosphere is composed of mainly nitrogen and methane (Niemann et al., 2010). The surface pressure is about 1125 Torr (1 Torr = 133.322 Pa) (Fulchignoni et al., 2005) and the methane abundance near the surface is about 5% but decreases to about 1.4% in the stratosphere (70–300 km) (Lellouch et al., 2014; Niemann et al., 2010). The production of organic molecules begins high in the atmosphere by the dissociation and ionization of nitrogen and methane by UV radiation and energetic particles to form species such as CH_3, N and N^+ (Vuitton et al., 2008). A wide variety of subsequent reactions produce a complex mixture of species; for example, C_2H_6 is produced primarily by the reaction of two CH_3 radicals (Yung et al., 1984a). These radical-radical combination reactions, along with other photochemical processes, allow for the formation of larger hydrocarbons; indeed, benzene has been observed on Titan (Coustenis et al., 2007), and benzene can undergo further photochemistry to generate large, complex aromatic species (Jennings et al., 2017; Vuitton et al., 2008).

Much of what is known about Titan's atmosphere comes from the Cassini-Huygens mission, which lasted for 13 years in orbit around Saturn. To date, in addition to CH_4 and N_2, 19 neutral molecules have been detected on Titan (see Table 1 of (Hörst, 2017)); of these, 15 have been measured with the Composite Infrared Spectrometer, CIRS, on Cassini (Jennings et al., 2017). CIRS covers the 10–1500 cm^{-1} spectral range at a maximum spectral resolution of 0.5 cm^{-1}. In order to interpret the CIRS thermal emission spectra of Titan (as well as those of Jupiter and Saturn) to obtain molecular abundances, laboratory spectral data are required. For the smaller molecules such as CH_4, suitable line parameters including pressure broadening coefficients at low temperature are needed, while for larger molecules absorption cross sections covering the range of planetary temperature, pressure and composition

* Corresponding author.
E-mail address: dhewett@odu.edu (D. Hewett).

https://doi.org/10.1016/j.icarus.2019.113460
Received 31 January 2019; Received in revised form 10 September 2019; Accepted 1 October 2019
Available online 21 October 2019

are necessary. The Bernath group has recently published infrared absorption cross sections for propane broadened by hydrogen and helium at low temperatures (Wong et al., 2018; Wong et al., 2017a; Wong et al., 2017b) suitable for the Giant Planets. Sung et al. (2018) have reported infrared cross sections of propene broadened by nitrogen to improve the detection of propene on Titan (Nixon et al., 2013; Lombardo et al., 2019a). Conducting these laboratory studies in atmospherically relevant conditions, such as temperature and the presence of broadening gases (hydrogen, helium, and nitrogen), is essential to provide accurate spectra for comparison with astronomical observations.

The work reported below focuses on the 1050–1900 cm^{-1} spectral region of isobutane. Isobutane $HC(CH_3)_3$ has not yet been detected in Titan's atmosphere, although formation of C_4H_{10} has been predicted with photochemical models generally without distinguishing between the *n*-butane ($CH_3CH_2CH_2CH_3$) and isobutane isomers (Dobrijevic et al., 2016; Vuitton et al., 2019; Yung et al., 1984b). Dobrijevic et al. (2016) predict that C_4H_{10} is as abundant as propane, which has already been detected (Nixon et al., 2009; Maguire et al., 1981). However, in an experimental simulation of the chemistry in Titan's atmosphere, *n*-butane production was favored over isobutane (Tran et al., 2005).

The primary pathway suggested by Vuitton et al. for generating butane on Titan involves radical-radical recombination of a propyl radical and a methyl radical. There are two isomers of the propyl radical, the primary radical and the secondary radical, where radical-radical recombination between a methyl radical and a primary propyl radical would result in *n*-butane, whereas combination of the secondary propyl radical and a methyl radical would generate isobutane. Since a secondary radical is more stable, it is reasonable to assume that most of the propyl radicals would be secondary, suggesting that most of the C_4H_{10} generated in Titan's atmosphere would be isobutane. This argument does not agree with the results of Tran et al. (2005) but does agree with Coll et al., who find that isobutane should be present in greater abundance (Coll et al., 1999).

The equilibrium structure of isobutane has C_{3v} symmetry (Lide, 1960), with 24 fundamental vibrational frequencies (Manzanares et al., 1995), 8 with a_1 symmetry, 4 nominally forbidden a_2 modes (ν_9-ν_{12}) and 12 doubly degenerate e modes (ν_{13}-ν_{24}). There are two weak low frequency torsional modes ν_{12} (a_2) at 225 cm^{-1} and ν_{24} (e) at 280 cm^{-1} (Weiss and Leroi, 1969). Infrared absorption cross sections of isobutane are available from the Pacific Northwest National Laboratory (PNNL) recorded at 0.1 cm^{-1} resolution from 600 to 6500 cm^{-1} with 1 atm of N_2 at 5, 25, 50 °C (Sharpe et al., 2004). Most of the PNNL infrared absorption cross sections are now available in the HITRAN database (https://hitran.org/). Recently we have recorded high resolution absorption cross sections in the 3 μm region at low temperatures with H_2 and N_2 as broadening gases (Hewett et al., 2019) and we now extend this work to longer wavelengths.

2. Experimental

The experimental setup used in this study has been described in detail elsewhere, and therefore only a brief description will be given here (Hewett et al., 2019; Wong et al., 2017b). The isobutane data were taken at the Canadian Light Source (CLS) far-infrared beamline using a 2-meter base path White-type multipass cell coupled with a Bruker IFS 125 HR spectrometer fitted with a KBr beam splitter. The total path length was 8.63 ± 0.02 m. A Neslab ULT-80DD refrigerated recirculating methanol bath was used to cool the cell, and a liquid helium cooled Ge:Cu bolometer detector was used with either the internal glowbar of the spectrometer or the synchrotron radiation. The cell temperature was monitored with PT100 RTD sensors with an estimated accuracy of ±2 K. The isobutane pressure was measured with a 10 Torr Baratron pressure gauge, and the total pressure including the broadening gas was measured with a 1000 Torr Baratron pressure gauge. Each spectrum is the average of a minimum of 400 interferograms, with a boxcar apodization function and a zero-filling factor of 8.

The spectral resolutions (using the Bruker definition of 0.9/optical path difference) were 0.00096, 0.005, 0.01, 0.04 cm^{-1} for the pure sample, 10 Torr, 30 Torr and 100 Torr experiments, respectively. The pressures of butane were chosen to provide substantial signal without saturating any of the relevant bands. The relative abundancies range from 1 in the pure spectra down to ~0.001 for the 100 Torr broadening gas measurements (Table 1). To save time, the background spectra were all recorded at 0.04 cm^{-1} resolution, except for the pure sample which had a 0.015 cm^{-1} resolution background.

Spectra were recorded for 4 temperatures: nominally 210 K, 234 K, 265 K and 296 K. Although it is desirable to go to lower temperatures to match stratospheric temperatures on Titan and the Giant Planets more closely, the minimum temperature was limited by the Neslab chiller. At each temperature 3 pressures of the broadening gas (N_2 or H_2) were used: nominally 10 Torr, 30 Torr and 100 Torr; in addition, spectra of pure samples were also recorded. The temperature and pressure parameters used during data collection are shown in Table 1. The pressure listed for the broadening gas (N_2 or H_2) is in fact the total pressure in the cell.

2.1. Calibration

Due to potential inaccuracies of the pressure gauges, a calibration may be needed to obtain accurate absorption cross sections. The Pacific Northwest National Laboratory (PNNL) database (Sharpe et al., 2004) has over four hundred vapor-phase infrared spectra which can be used for comparison. The PNNL spectra are reported at 3 sample temperatures (278, 298 and 323 K) with 1 atm of N_2 broadening gas. The integrated area of the absorption cross sections of isolated bands are not highly dependent on temperature (Ballard et al., 2000; Orlando et al., 1992) and can be used for calibration.

The CLS transmission spectra are converted to cross sections using the Beer-Lambert law as written with a correction factor ξ in Harrison et al. (2010):

$$\sigma(\nu, T) = -\xi \frac{10^4 k_B T}{Pl} ln\tau(\nu, T)$$

In which $\tau(\nu, T)$ is the transmittance at wavenumber ν (cm^{-1}) and temperature T (K), P is the pressure of the absorbing gas in pascals (Pa), l is the optical path length (m), and k_B is the Boltzmann constant ($1.3806504 * 10^{-23}$ J/K). ξ is the correction (calibration) factor relative to the PNNL average value. The PNNL integrated values, integrating over the bands from 1301.43 cm^{-1} to 1572.23 cm^{-1}, are as follows: 7.518×10^{-18} cm/molecule at 5 °C, 7.43973×10^{-18} cm/molecule at

Table 1
Pressures and temperatures for each isobutane (IB) measurement.

H_2			N_2			Pure	
IB P (Torr)	H_2 P (Torr)	T (K)	IB P (Torr)	N_2 P (Torr)	T (K)	IB P (Torr)	T (K)
210 K							
0.101	9.9	209.35	0.093	9.98	210.05	0.050	208.85
0.099	30.1	210.15	0.093	30.1	210.25		
0.121	100.5	210.35	0.119	99.8	210.25		
234 K							
0.103	10.2	234.15	0.114	10.1	234.25	0.089	234.25
0.160	30.4	234.15	0.135	29.7	234.25		
0.226	99.8	234.25	0.221	99.8	234.25		
265 K							
0.195	10.4	265.25	0.199	9.98	265.35	0.125	265.25
0.191	30	265.25	0.190	30.2	265.75		
0.205	99.8	265.25	0.207	99.8	265.75		
296 K							
0.244	10.4	295.55	0.219	10.2	295.75	0.250	294.55
0.300	30.2	295.65	0.301	30.0	295.65		
0.360	99.8	295.75	0.400	99.8	295.75		

25 °C, and 7.32522×10^{-18} cm/molecule at 50 °C, for an average value of 7.42765×10^{-18} cm/molecule.

The zero level of the baselines of the cross sections were corrected with the help of the PNNL data. The correction factor ξ for each spectrum was calculated by taking the ratio between the integrated area of the PNNL absorption spectra and the integrated area of all of the CLS absorption spectra from this study. The average value for ξ was 1.276 ± 0.016 (two sigma). As discussed below, this "correction factor, ξ" is unreasonable and we used a value of 1 in our analysis. The resolution was set to fully resolve the absorption features and the isobutane pressures were adjusted (Table 1) so that none of the features, including the Q-branch at 1478 cm^{-1} (Fig. 1), were saturated.

Starting in 2010 (Harrison et al., 2010, Harrison and Bernath, 2010), we have calibrated our high resolution cross sections with PNNL data and our values typically differ by 5–10%. A difference of nearly 30% for isobutane is without precedent, except for a similar large value for isobutane in the 3.3 μm region (Hewett et al., 2019). We have also not experienced any problems with the Baratron pressure gauges at the CLS. In addition, we have recorded spectra of isobutane at Old Dominion University in the 3.3 μm region and found a similar but slightly larger discrepancy with PNNL cross sections. As a result, we think that there is likely a problem with the intensity calibration of PNNL data for isobutane and have adopted the measured CLS pressures for our analysis (i.e., $\xi = 1$ for all spectra). The final cross section files are available in the section Appendix A. Supplementary Materials.

An overview spectrum is presented (Fig. 1) with isobutane at 210.05 K with 9.98 Torr of N_2 broadening gas. Weak residual impurity water lines from the ν_2 bending mode are present and some of the spectra have small residual channeling from imperfect cancellation of interference fringes. The mode assignments are taken from Bernath et al. (2019). Several of the bands have resolved rotational structure that has been analyzed in a separate publication (Bernath et al., 2019). Figs. 2 and 3 show the pressure and temperature dependencies on the spectra, respectively.

The accuracy of PNNL cross sections is estimated as ±3.2% (2 standard deviations) based on typical statistical noise and a comparison of independent measurements carried out at PNNL and NIST (Sharpe et al., 2004). However, we find an average bias of $27.6 \pm 1.8\%$ (2 sigma), i.e., the PNNL cross sections need to be divided by 1.276 or multiplied by 0.783 to bring them into agreement with our measurements. This means that our measurement precision for intensities is about 2% (2 sigma), based on the 1.8% variability relative to PNNL. The continuum signal-to-noise ratios for the transmission spectra range from 350 to 1150 except for the pure spectra for which they range from 100 to 160. The errors are therefore dominated by a number of systematic effects discussed in more detail by Harrison et al. (2010). Systematic errors are very difficult to estimate, except by comparison with independent measurements. Unfortunately, the only independent measurements we have at the moment are from PNNL, which are not reliable for isobutane. The two sigma accuracy for similar measurements of ethane cross sections was estimated to be 8% (Harrison et al., 2010), which is a typical value for our cross section measurements. Thus based on previous work (Harrison et al., 2010) and our experience, we estimate a total error of about 10% (two sigma) for the cross sections.

The calibration of the wavenumber scale was checked by comparing water lines in the spectra to the values in the HITRAN database (Gordon et al., 2017). The line positions were within 0.0005 cm^{-1} and therefore no wavenumber calibration was performed.

3. Butane on Titan

3.1. CIRS data

The Composite Infrared Spectrometer (CIRS) was a Fourier transform spectrometer on the Cassini spacecraft that explored the Saturnian system from 2004 through 2017 (Jennings et al., 2017). During the Cassini mission, the spacecraft performed 127 flybys of Titan, many of which included CIRS observations. We employ data from Focal Plane 4 (FP4) of CIRS, sensitive to the region from 1100 cm^{-1} to 1500 cm^{-1}. Data were acquired in a limb-viewing geometry and include spectra with tangent altitudes between 200 and 250 km above Titan's equatorial region from 30° S to 30° N between 2007 and 2017, including a total of 1555 individual spectra. Limb observations were utilized in this search to make use of long path length observations – by looking through atmosphere as

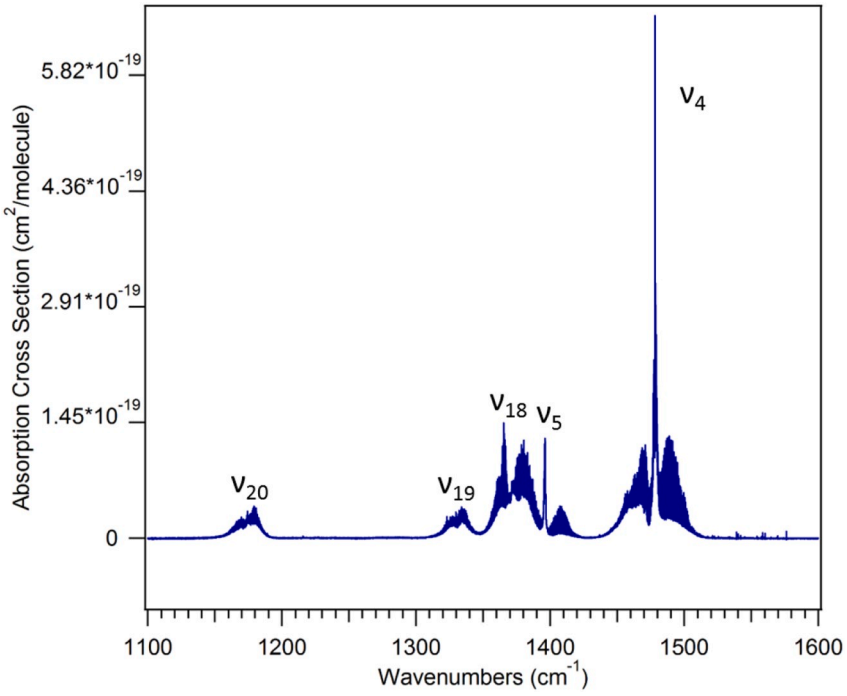

Fig. 1. An overview of the isobutane absorption cross sections at 210.05 K with 9.98 Torr of N_2 broadening gas. Water impurity water lines are visible from 1500 to 1600 cm^{-1}.

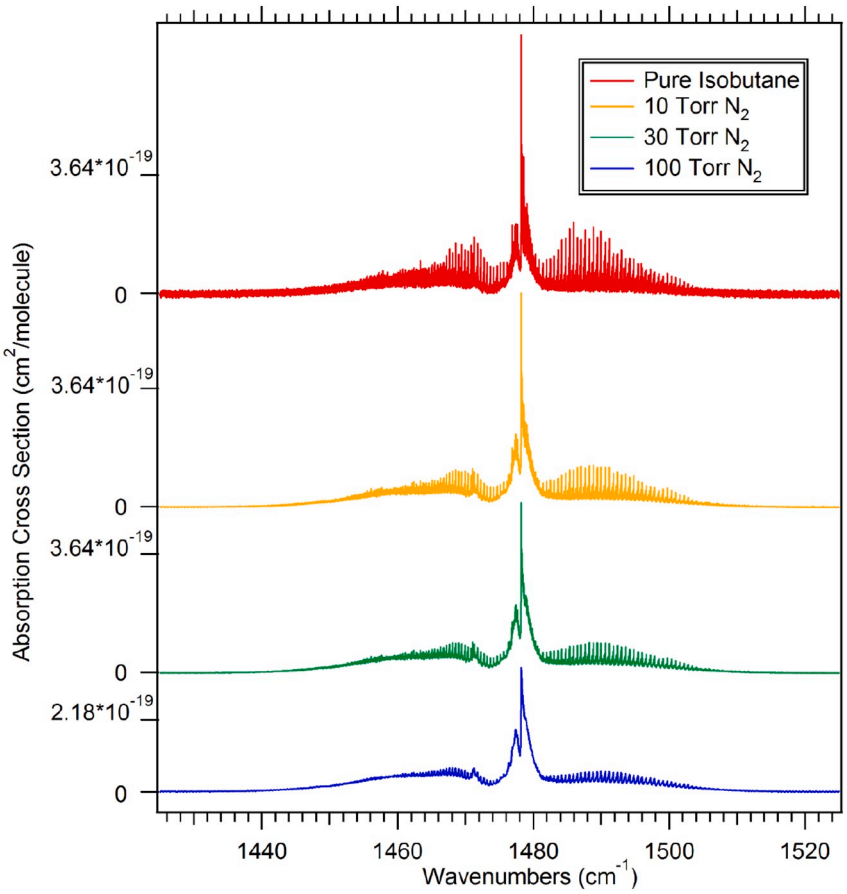

Fig. 2. Pressure series of the ν_4 band of isobutane at 209 K with N_2 as a broadening gas.

opposed to staring at the surface, we are able to isolate emission from higher altitudes where trace species are expected to exist in higher concentrations, as well as collect more radiation emitted by these molecules. However, if we look too high, the atmospheric pressure decreases to the point where molecular emission could not be detected by these observations. The resolution of the data is 0.5 cm^{-1}; however, we make use of over-sampled data at a resolution of 0.25 cm^{-1} to better distinguish weak features in the spectrum.

3.2. Modeling

We model the spectrum using the Nonlinear Optimal Estimator for Multispectral Analysis (NEMESIS) inverse radiative transfer algorithm (Irwin et al., 2008). NEMESIS has been used extensively to model infrared spectra of outer Solar System bodies previously; the reader is directed to (Lombardo et al., 2019a) and references therein for further discussion of the modeling method.

Our analysis proceeds by first determining the thermal structure of Titan's stratosphere over the duration of these observations. Stratospheric methane is well constrained in abundance, thus we can model the ν_4 band of methane from 1275 cm^{-1} to 1325 cm^{-1} by only varying the temperature and aerosol abundance (contributing only to the continuum of the spectrum) to best fit the observations.

The strongest isobutane band in the CIRS range is $\nu_4(a_1)$, which has a sharp Q-branch at 1478 cm^{-1} (Fig. 1). The strongest *n*-butane bands in the CIRS range are $\nu_{31}(b_u)$, $\nu_{30}(b_u)$ and $\nu_{14}(a_u)$ at 1462, 1466 and 1471 cm^{-1}, respectively, for the *s-trans* conformer of C_{2h} symmetry (Durig et al., 1991; Sharpe et al., 2004). However, due to the fact that beyond approximately 1400 cm^{-1} CIRS spectra become affected by aliasing from higher wavenumbers due to the FTS nature of the instrument, we model the region from 1440 to 1480 cm^{-1}. This spectral region has been successfully modeled previously by Lombardo et al. (2019a, 2019b).

Since we do not have spectral line lists for butane and isobutane, we make use of the same method described in Nixon et al., 2013. We model as best we can the spectrum including spectral line lists for all species known to emit in this region - ethane, propane, and aerosol haze. Spectral line data for methane and ethane are from HITRAN 2016 (Gordon et al., 2017), spectral data for propane are from Sung et al. (2013) and the spectral characteristics of the aerosol haze are those defined in Vinatier et al. (2012). After we have successfully modeled the spectrum, we compare the residual – the difference between the observations and the model – to the laboratory spectra for butane and isobutane. If no significant emission is seen in the residual, we can proceed to calculate an upper-limit for the species using the method described in the following section.

3.3. Modeling results

Results of the spectral fitting are shown in Fig. 4. The region of the CIRS spectrum past ~1400 cm^{-1} is difficult to model due to many broad overlapping bands (notably from methane, ethane and propane), contributions from potentially undetected species, and aliasing from higher wavenumbers.

We do not detect isobutane with the CIRS spectra but can compute an upper-limit for its abundance. As described in Nixon et al. (2013), the spectral radiance of optically thin molecular emission lines is proportional to the molecular abundance (q), absorption cross section (k), and the temperature and pressure at the source of emission (T and p). Due to the difference in temperature between Titan's stratosphere (T_T, 150 K) and the laboratory environment at which the absorption cross sections were calculated (T_L, 278 K for PNNL and 210 K for isobutane), we

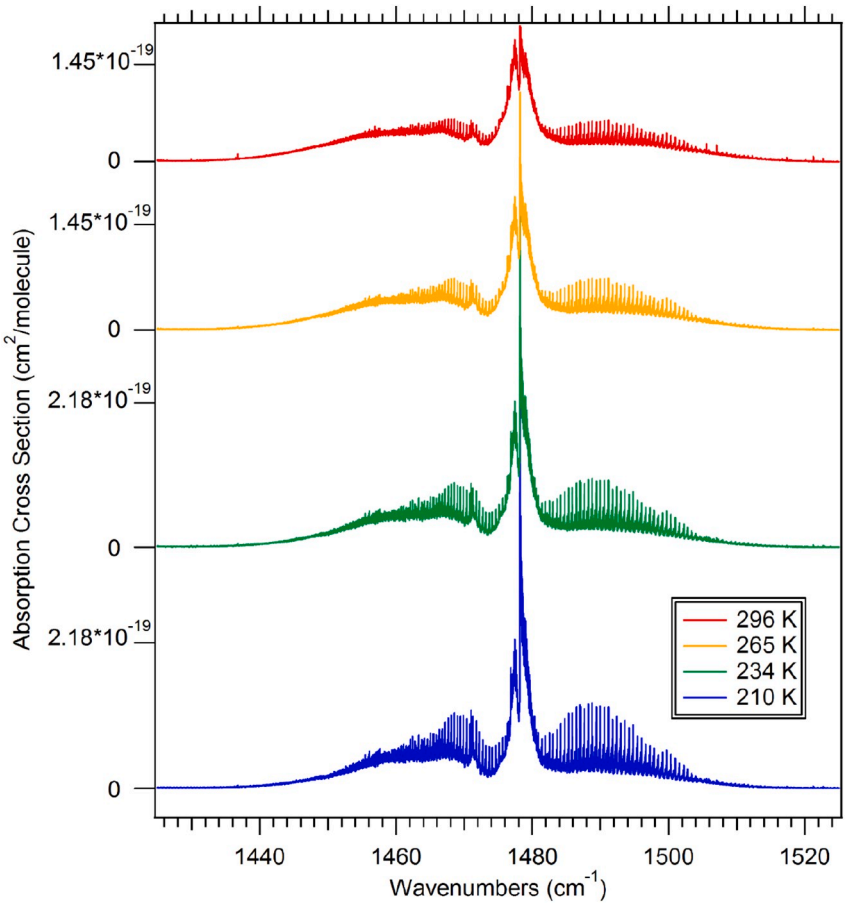

Fig. 3. Temperature series of the ν_4 band of isobutane at 10 Torr N_2 as a broadening gas.

include a first order correction factor:

$$f(v, T_T, T_L) = \frac{exp(-c_2 v/T_T)/V(T_T)}{exp(-c_2 v/T_L)/V(T_L)}$$

where $c_2 = hc/k = 1.4388$ cm K, and $V(T)$ is the vibrational partition function of the molecule. Note that the PNNL cross section data used were recorded at 278 K but provided in units of ppm^{-1} m^{-1} at 296 K; conversion to cm^2/molecule units requires multiplication by 9.28697×10^{-16} cm^2 mol^{-1} ppm m. The vibrational partition functions were calculated assuming the harmonic oscillator approximation with the vibrational frequencies for *n*-butane taken from Durig et al. (1991) and those for isobutane from Manzanares et al. (1995).

If we denote the Planck function at wavenumber ν and temperature T_T as $B(\nu, T_T)$, we can write that

$$I(v) \propto k(v)\, f(v)\, q\, p\, B(v, T_T),$$

where I(ν) is the brightness of the molecular emission. To estimate the upper limit of isobutane, we take the ratio of this equation between the brightest line of the isobutane spectrum and a prominent line in the CIRS spectrum - in our case the 1468.50 cm^{-1} ethane line - and rearrange to solve for q

$$q_{C_4H_{10_{max}}} = q_{C_2H_6} \frac{k_{C_2H_6}}{k_{C_4H_{10}}} \frac{f(C_2H_6, T_T, T_L)}{f(C_4H_{10}, T_T, T_L)} \frac{\text{spectral error}}{I_{C_2H_6}}$$

We use the same method to calculate an upper-limit for *n*-butane, using laboratory cross sections from the PNNL. Values used in these calculations are given in Table 2.

We calculate a 3-σ upper limit of *n*-butane of 5.13e-7, and isobutane of 3.91e-8. The sum of these values, 5.52e-7 is consistent with predicted abundance of both isomers presented in (Dobrijevic et al., 2016), who predict a stratospheric abundance in the range (2−10)e-7.

4. Discussion and conclusion

Isobutane spectra were collected over a wide range of temperatures and broadening gas pressures in order to simulate the various conditions present in the atmospheres of Titan, Jupiter and Saturn. The atmospheres of Jupiter and Saturn are primarily composed of hydrogen, while the primary component of Titan's atmosphere is nitrogen, making hydrogen and nitrogen the logical choices for broadening gases.

The changes in the spectrum due to varying broadening gas pressure and temperature can be seen in Figs. 3 and 4, respectively. As the pressure of the broadening gas is increased, a decrease in the resolution is observed due to pressure broadening. A similar trend is observed in the temperature series, where the resolution decreases as the temperature increases from Doppler broadening and hot bands.

Although butane is predicted by chemical models to be detectable in Titan's atmosphere, we derive only upper limits for isobutane (3.91e-8), *n*-butane (5.13e-7) and both isomers (5.52e-7). Our upper limits are consistent with the lower limit of the abundance range of butane predicted by the detailed model of Dobrijevic et al. (2016).

A series of isobutane spectra were recorded to provide astronomers a catalog with which to make accurate simulations of astronomical spectra. These data were used to determine an upper abundance limit for isobutane in Titan's atmosphere with CIRS spectra. Upper limits were also determined for *n*-butane using PNNL cross sections and the butane upper limits are consistent with the lower limit of predictions of state-of-the-art chemical models of Titan's atmosphere.

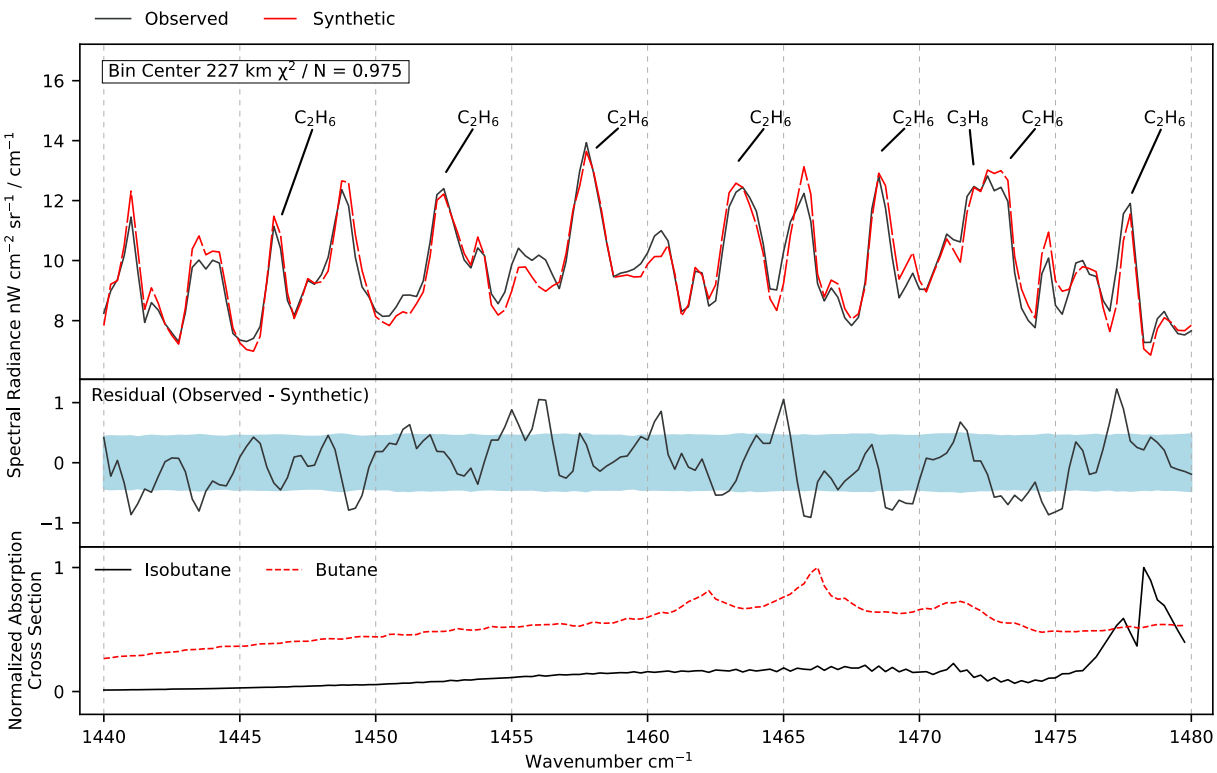

Fig. 4. The top plot shows the synthetic spectrum (dashed red) compared to the observed spectrum (solid black). Major molecule contributions are labeled, unlabeled lines are weaker emission from ethane. The residual (middle plot) is the difference between the observed and modeled spectra – a positive value indicates excess emission in the observation that is not being properly modeled. The blue envelope is a 1-σ estimate of the error on the spectrum, including instrumental and systematic error, derived from the standard deviation of the spectrum. The bottom plot shows the laboratory spectra for isobutane from this work (solid black) and *n*-butane from PNNL (red dashed), normalized over this spectral window for clarity and convolved with a Hamming function of full width at half maximum of 0.475 cm^{-1} to match the CIRS resolution. The PNNL *n*-butane cross sections are for 5 °C and 1 atm of N_2 and the isobutane data are for 210 K with 100 Torr of N_2. (For interpretation of the references to colour in this figure legend, the reader is referred to the web version of this article.)

Table 2
Values used in the butane and isobutane upper-limit calculations. Values marked with a single asterisk (*) are the spectral error on the observations, multiplied by $3\sqrt{2}$ to account for oversampling of the data and conversion from 1-σ spectral error to 3-σ upper-limit.

Molecule	*f*	*ν*, cm^{-1}	k, cm^2/molecule	I (nW)	q
C_2H_6	0.00205	1468.50	7.5e-20	5.8	1.0e-5
n-C_4H_{10}	0.00657	1466.25	1.0e-19	1.26*	<5.13e-7
i-C_4H_{10}	0.0291	1478.25	3.0e-19	1.28*	<3.91e-8

Acknowledgements

The NASA Outer Planets Research and Planetary Data Archiving and Restoration Tools program (PDART) provided funding. We thank M. Pokhrel for help with the analysis. Research described in this paper was performed at the Canadian Light Source, which is supported by the Canada Foundation for Innovation, Natural Sciences and Engineering Research Council of Canada, the University of Saskatchewan, the Government of Saskatchewan, Western Economic Diversification Canada, the National Research Council Canada, and the Canadian Institutes of Health Research. The authors (NAL, CAN and DEJ) appreciate support from NASA's Cassini mission and the Cassini Data Analysis Program.

Appendix A. Supplementary data

Supplementary data to this article can be found online at https://doi.org/10.1016/j.icarus.2019.113460.

References

Ballard, J., Knight, R.J., Newnham, D.A., Auwera, J.V., Herman, M., Lonardo, G.D., Masciarelli, G., Nicolaisen, F.M., Beukes, J.A., Christensen, L.K., McPheat, R., Duxbury, G., Freckleton, R., Shine, K.P., 2000. An intercomparison of laboratory measurements of absorption cross-sections and integrated absorption intensities for HCFC-22. J. Quant. Spectrosc. Radiat. Transf. 66 (2), 109–128. https://doi.org/10.1016/S0022-4073(99)00211-3.

Bernath, P.F., Bittner, D.M., Sibert III, E.L., 2019. Isobutane infrared bands: partial rotational assignments, ab initio calculations and local mode analysis. J. Phys. Chem. A. https://doi.org/10.1021/acs.jpca.9b03321 in press.

Bezard, B., 2009. Composition and chemistry of Titan's stratosphere. Philosophical Transactions of the Royal Society a-Mathematical Physical and Engineering Sciences 367 (1889), 683–695. https://doi.org/10.1098/rsta.2008.0186.

Bezard, B., Yelle, R.V., Nixon, C.A., 2014. The composition of Titan's atmosphere. In: Titan: Interior, Surface, Atmosphere, and Space Environment, 14, pp. 158–189.

Coll, P., Coscia, D., Smith, N., Gazeau, M.C., Ramírez, S.I., Cernogora, G., Israël, G., Raulin, F., 1999. Experimental laboratory simulation of Titan's atmosphere: aerosols and gas phase. Planetary and Space Science 47 (10), 1331–1340. https://doi.org/10.1016/S0032-0633(99)00054-9.

Coustenis, A., Achterberg, R.K., Conrath, B.J., Jennings, D.E., Marten, A., Gautier, D., Nixon, C.A., Flasar, F.M., Teanby, N.A., Bezard, B., Samuelson, R.E., Carlson, R.C., Lellouch, E., Bjoraker, G.L., Romani, P.N., Taylor, F.W., Irwin, P.G.J., Fouchet, T., Hubert, A., Orton, G.S., Kunde, V.G., Vinatier, S., Mondellini, J., Abbas, M.M., Courtin, R., 2007. The composition of Titan's stratosphere from Cassini/CIRS mid-infrared spectra. Icarus 189 (1), 35–62. https://doi.org/10.1016/j.icarus.2006.12.022.

Dobrijevic, M., Loison, J.C., Hickson, K.M., Gronoff, G., 2016. 1d-coupled photochemical model of neutrals, cations and anions in the atmosphere of Titan. Icarus 268, 313–339. https://doi.org/10.1016/j.icarus.2015.12.045.

Durig, J.R., Wang, A., Beshir, W., Little, T.S., 1991. Barrier to asymmetric internal rotation, conformational stability, vibrational spectra and assignments, and ab initio calculations of n-butane-d0, d5 and d10. J. Raman Spectrosc. 22 (11), 683–704. https://doi.org/10.1002/jrs.1250221115.

Flasar, F.M., Achterberg, R.K., Conrath, B.J., Gierasch, P.J., Kunde, V.G., Nixon, C.A., Bjoraker, G.L., Jennings, D.E., Romani, P.N., Simon-Miller, A.A., Bezard, B., Coustenis, A., Irwin, P.G.J., Teanby, N.A., Brasunas, J., Pearl, J.C., Segura, M.E., Carlson, R.C., Mamoutkine, A., Schinder, P.J., Barucci, A., Courtin, R., Fouchet, T., Gautier, D., Lellouch, E., Marten, A., Prange, R., Vinatier, S., Strobel, D.F., Calcutt, S.

B., Read, P.L., Taylor, F.W., Bowles, N., Samuelson, R.E., Orton, G.S., Spilker, L.J., Owen, T.C., Spencer, J.R., Showalter, M.R., Ferrari, C., Abbas, M.M., Raulin, F., Edgington, S., Ade, P., Wishnow, E.H., 2005. Titan's atmospheric temperatures, winds, and composition. Science 308 (5724), 975–978. https://doi.org/10.1126/science.1111150.

Fulchignoni, M., Ferri, F., Angrilli, F., Ball, A.J., Bar-Nun, A., Barucci, M.A., Bettanini, C., Bianchini, G., Borucki, W., Colombatti, G., Coradini, M., Coustenis, A., Debei, S., Falkner, P., Fanti, G., Flamini, E., Gaborit, V., Grard, R., Hamelin, M., Harri, A.M., Hathi, B., Jernej, I., Leese, M.R., Lehto, A., Stoppato, P.F.L., Lopez-Moreno, J.J., Makinen, T., McDonnell, J.A.M., McKay, C.P., Molina-Cuberos, G., Neubauer, F.M., Pirronello, V., Rodrigo, R., Saggin, B., Schwingenschuh, K., Seiff, A., Simoes, F., Svedhem, H., Tokano, T., Towner, M.C., Trautner, R., Withers, P., Zarnecki, J.C., 2005. In situ measurements of the physical characteristics of Titan's environment. Nature 438 (7069), 785–791. https://doi.org/10.1038/nature04314.

Gordon, I.E., Rothman, L.S., Hill, C., Kochanov, R.V., Tan, Y., Bernath, P.F., Birk, M., Boudon, V., Campargue, A., Chance, K.V., Drouin, B.J., Flaud, J.M., Gamache, R.R., Hodges, J.T., Jacquemart, D., Perevalov, V.I., Perrin, A., Shine, K.P., Smith, M.A.H., Tennyson, J., Toon, G.C., Tran, H., Tyuterev, V.G., Barbe, A., Császár, A.G., Devi, V. M., Furtenbacher, T., Harrison, J.J., Hartmann, J.M., Jolly, A., Johnson, T.J., Karman, T., Kleiner, I., Kyuberis, A.A., Loos, J., Lyulin, O.M., Massie, S.T., Mikhailenko, S.N., Moazzen-Ahmadi, N., Müller, H.S.P., Naumenko, O.V., Nikitin, A. V., Polyansky, O.L., Rey, M., Rotger, M., Sharpe, S.W., Sung, K., Starikova, E., Tashkun, S.A., Auwera, J.V., Wagner, G., Wilzewski, J., Wcisło, P., Yu, S., Zak, E.J., 2017. The Hitran 2016 molecular spectroscopic database. J. Quant. Spec. Rad. Trans. 203, 3–69. https://doi.org/10.1016/j.jqsrt.2017.06.038.

Harrison, J.J., Bernath, P.F., 2010. Infrared absorption cross sections for propane (C_3H_8) in the 3 μm region. J. Quant. Spec. Rad. Trans. 111 (9), 1282–1288. https://doi.org/10.1016/j.jqsrt.2009.11.027.

Harrison, J.J., Allen, N.D.C., Bernath, P.F., 2010. Infrared absorption cross sections for ethane (C_2H_6) in the 3 μm region. J. Quant. Spec. Rad. Trans. 111 (3), 357–363. https://doi.org/10.1016/j.jqsrt.2009.09.010.

Hewett, D.M., Bernath, P.F., Billinghurst, B.B., 2019. Infrared absorption cross sections of isobutane with hydrogen and nitrogen as broadening gases. J. Quant. Spec. Rad. Trans. 227, 226–229. https://doi.org/10.1016/j.jqsrt.2019.02.008.

Hörst, S.M., 2017. Titan's atmosphere and climate. J. Geophys. Res. Plan. 122 (3), 432–482. https://doi.org/10.1002/2016JE005240.

Irwin, P.G.J., Teanby, N.A., de Kok, R., Fletcher, L.N., Howett, C.J.A., Tsang, C.C.C., Wilson, C.F., Calcutt, S.B., Nixon, C.A., Parrish, P.D., 2008. The nemesis planetary atmosphere radiative transfer and retrieval tool. J. Quant. Spec. Rad. Trans. 109 (6), 1136–1150. https://doi.org/10.1016/j.jqsrt.2007.11.006.

Jennings, D.E., Flasar, F.M., Kunde, V.G., Nixon, C.A., Segura, M.E., Romani, P.N., Gorius, N., Albright, S., Brasunas, J.C., Carlson, R.C., Mamoutkine, A.A., Guandique, E., Kaelberer, M.S., Aslam, S., Achterberg, R.K., Bjoraker, G.L., Anderson, C.M., Cottini, V., Pearl, J.C., Smith, M.D., Hesman, B.E., Barney, R.D., Calcutt, S., Vellacott, T.J., Spilker, L.J., Edgington, S.G., Brooks, S.M., Ade, P., Schinder, P.J., Coustenis, A., Courtin, R., Michel, G., Fettig, R., Pilorz, S., Ferrari, C., 2017. Composite infrared spectrometer (CIRS) on Cassini. Appl. Opt. 56 (18), 5274–5294. https://doi.org/10.1364/AO.56.005274.

Lebonnois, S., Toublanc, D., Hourdin, F., Rannou, P., 2001. Seasonal variations of Titan's atmospheric composition. Icarus 152 (2), 384–406. https://doi.org/10.1006/icar.2001.6632.

Lellouch, E., Bezard, B., Flasar, F.M., Vinatier, S., Achterberg, R., Nixon, C.A., Bjoraker, G.L., Gorius, N., 2014. The distribution of methane in Titan's stratosphere from Cassini/CIRS observations. Icarus 231, 323–337. https://doi.org/10.1016/j.icarus.2013.12.016.

Lide, D.R., 1960. Structure of the isobutane molecule; change of dipole moment on isotopic substitution. J. Chem. Phys. 33 (5), 1519–1522. https://doi.org/10.1063/1.1731435.

Lombardo, N.A., Nixon, C.A., Achterberg, R.K., Jolly, A., Sung, K., Irwin, P.G.J., Flasar, F. M., 2019a. Spatial and seasonal variations in C_3H_x hydrocarbon abundance in Titan's stratosphere from Cassini CIRS observations. Icarus 317, 454–469. https://doi.org/10.1016/j.icarus.2018.08.027.

Lombardo, N.A., Nixon, C.A., Sylvestre, M., Jennings, D.E., Teanby, N., Irwin, P.J.G., Flasar, F.M., 2019b. Ethane in Titan's stratosphere from Cassini CIRS far- and mid-infrared spectra. Astron. J. 157, 160. https://doi.org/10.3847/1538-3881/ab0e07.

Maguire, W.C., Hanel, R.A., Jennings, D.E., Kunde, V.G., Samuelson, R.E., 1981. C_3H_8 and C_3H_4 in Titan's atmosphere. Nature 292, 683–686. https://doi.org/10.1038/292683a0.

Manzanares, C., Peng, J., Mina-Camilde, N., Brock, A., 1995. Overtone spectroscopy of isobutane at cryogenic temperatures. Chem. Phys. 190 (2), 247–259. https://doi.org/10.1016/0301-0104(94)00278-I.

Niemann, H.B., Atreya, S.K., Demick, J.E., Gautier, D., Haberman, J.A., Harpold, D.N., Kasprzak, W.T., Lunine, J.I., Owen, T.C., Raulin, F., 2010. Composition of Titan's lower atmosphere and simple surface volatiles as measured by the Cassini-Huygens probe gas chromatograph mass spectrometer experiment. Journal of Geophysical Research-Planets 115. https://doi.org/10.1029/2010je003659.

Nixon, C., Jennings D, E., Flaud, J.M., Bezard, B., A Teanby, N., Irwin, P., Anstty T, M., Coustenis, A., Vinatier, S., Flasar F, M., 2009. Titan's prolific propane: the Cassini CIRS perspective. Plan. Space Sci. 57 (13), 1573–1585. https://doi.org/10.1016/j.pss.2009.06.021.

Nixon, C.A., Jennings, D.E., Bézard, B., Vinatier, S., Teanby, N.A., Sung, K., Ansty, T.M., Irwin, P.G.J., Gorius, N., Cottini, V., Coustenis, A., Flasar, F.M., 2013. Detection of propene in Titan's stratosphere. The Astrophysical Journal Letters 776 (1), L14.

Orlando, J.J., Tyndall, G.S., Huang, A., Calvert, J.G., 1992. Temperature dependence of the infrared absorption cross sections of carbon tetrachloride. Geophys. Res. Lett. 19 (10), 1005–1008. https://doi.org/10.1029/91gl01036.

Rannou, P., McKay, C.P., Lorenz, R.D., 2003. A model of Titan's haze of fractal aerosols constrained by multiple observations. Planetary and Space Science 51 (14–15), 963–976. https://doi.org/10.1016/j.pss.2003.05.008.

Raulin, F., Gautier, D., Ip, W.H., 1984. Exobiology and the solar-system - the Cassini mission to Titan. Orig. Life Evol. Biosph. 14 (1–4), 817–824. https://doi.org/10.1007/bf00933738.

Raulin, F., Cerceau, F., Hakdaoui, M., Vargas, A., 1986. Prebiotic chemical evolution in Titan's ocean. Orig. Life Evol. Biosph. 16 (3–4), 401–402. https://doi.org/10.1007/bf02422097.

Sharpe, S.W., Johnson, T.J., Sams, R.L., Chu, P.M., Rhoderick, G.C., Johnson, P.A., 2004. Gas-phase databases for quantitative infrared spectroscopy. App. Spec. 58 (12), 1452–1461. https://doi.org/10.1366/0003702042641281.

Sung, K., Toon, G.C., Mantz, A.W., Smith, M.A.H., 2013. FT-IR measurements of cold C_3H_8 cross sections at 7–15 μm for Titan atmosphere. Icarus 226 (2), 1499–1513. https://doi.org/10.1016/j.icarus.2013.07.028.

Sung, K., Toon, G.C., Drouin, B.J., Mantz, A.W., Smith, M.A.H., 2018. FT-IR measurements of cold propene (C_3H_6) cross-sections at temperatures between 150 and 299 K. J. Quant. Spec. Rad. Trans. 213, 119–132. https://doi.org/10.1016/j.jqsrt.2018.03.011.

Teanby, N.A., Irwin, R.J., de Kok, R., Vinatier, S., Bezard, B., Nixon, C.A., Flasar, F.M., Calcutt, S.B., Bowles, N.E., Fletcher, L., Howett, C., Taylor, F.W., 2007. Vertical profiles of HCN, HC_3N, and C_2H_2 in Titan's atmosphere derived from Cassini/CIRS data. Icarus 186 (2), 364–384. https://doi.org/10.1016/j.icarus.2006.09.024.

Trainer, M.G., Pavlov, A.A., Jimenez, J.L., McKay, C.P., Worsnop, D.R., Toon, O.B., Tolbert, M.A., 2004. Chemical composition of Titan's haze: are PAHs present? Geophys. Res. Lett. 31 (17) https://doi.org/10.1029/2004gl019859.

Trainer, M.G., Pavlov, A.A., DeWitt, H.L., Jimenez, J.L., McKay, C.P., Toon, O.B., Tolbert, M.A., 2006. Organic haze on Titan and the early Earth. Proc. Natl. Acad. Sci. 103 (48), 18035–18042. https://doi.org/10.1073/pnas.0608561103.

Tran, B.N., Joseph, J.C., Force, M., Briggs, R.G., Vuitton, V., Ferris, J.P., 2005. Photochemical processes on Titan: irradiation of mixtures of gases that simulate Titan's atmosphere. Icarus 177 (1), 106–115. https://doi.org/10.1016/j.icarus.2005.03.015.

Vinatier, S., Bezard, B., Fouchet, T., Teanby, N.A., de Kok, R., Irwin, P.G.J., Conrath, B.J., Nixon, C.A., Romani, P.N., Flasar, E.M., Coustenis, A., 2007. Vertical abundance profiles of hydrocarbons in Titan's atmosphere at 15 degrees S and 80 degrees N retrieved from Cassini/CIRS spectra. Icarus 188 (1), 120–138. https://doi.org/10.1016/j.icarus.2006.10.031.

Vinatier, S., Bezard, B., Nixon, C.A., Mamoutkine, A., Carlson, R.C., Jennings, D.E., Guandique, E.A., Teanby, N.A., Bjoraker, G.L., Flasar, F.M., Kunde, V.G., 2010. Analysis of Cassini/CIRS limb spectra of Titan acquired during the nominal mission I. hydrocarbons, nitriles and CO_2 vertical mixing ratio profiles. Icarus 205 (2), 559–570. https://doi.org/10.1016/j.icarus.2009.08.013.

Vinatier, S., Rannou, P., Anderson, C.M., Bezard, B., de Kok, R., Samuelson, R.E., 2012. Optical constants of Titan's stratospheric aerosols in the 70-1500 cm^{-1} spectral range constrained by Cassini/CIRS observations. Icarus 219 (1), 5–12. https://doi.org/10.1016/j.icarus.2012.02.009.

Vuitton, V., Yelle, R.V., Cui, J., 2008. Formation and distribution of benzene on Titan. J. Geophys. Res. Plan. 113 (E5) https://doi.org/10.1029/2007JE002997.

Vuitton, V., Yelle, R.V., Klippenstein, S.J., Hörst, S.M., Lavvas, P., 2019. Simulating the density of organic species in the atmosphere of Titan with a coupled ion-neutral photochemical model. Icarus 324, 120–197. https://doi.org/10.1016/j.icarus.2018.06.013.

Weiss, S., Leroi, G.E., 1969. Infrared spectra and internal rotation in propane, isobutane and neopentane. Spec. Acta. A. Mol. Spec. 25 (11), 1759–1766. https://doi.org/10.1016/0584-8539(69)80204-7.

Wong, A., Billinghurst, B., Bernath, P.F., 2017a. Helium broadened propane absorption cross sections in the far-IR. Mol. Astrophys. 8, 36–39. https://doi.org/10.1016/j.molap.2017.06.003.

Wong, A., Hargreaves, R.J., Billinghurst, B., Bernath, P.F., 2017b. Infrared absorption cross sections of propane broadened by hydrogen. J. Quant. Spec. Rad. Trans. 198, 141–144. https://doi.org/10.1016/j.jqsrt.2017.05.006.

Wong, A., Appadoo, D.R.T., Bernath, P.F., 2018. IR absorption cross sections of propane broadened by H2 and He between 150 K and 210 K. J. Quant. Spec. Rad. Trans. 218, 68–71. https://doi.org/10.1016/j.jqsrt.2018.06.026.

Yung, Y.L., Allen, M., Pinto, J.P., 1984a. Photochemistry of the atmosphere of Titan - comparison between model and observations. Astrophys. J. Suppl. Ser. 55 (3), 465–506. https://doi.org/10.1086/190963.

Yung, Y.L., Allen, M., Pinto, J.P., 1984b. Photochemistry of the atmosphere of Titan: comparison between model and observations. Astrophys. J. Suppl. Ser. 55 (3), 465–506.